Tween–80 Coating in Enhancing Physicochemical Stability, Kinetics and Release Mechanism of Layered Double Hydroxide-Ferulate

Sharifah Norain Mohd Sharif[1,2*], Norhayati Hashim[1,2], Illyas Md Isa[1,2], Maizatul Najwa Jajuli[1,2], Afif Arifin[3], Norlaili Abu Bakar[1], Mazidah Mamat[4], and Suyanta Suyanta[5]

[1]*Department of Chemistry, Faculty of Science and Mathematics, Universiti Pendidikan Sultan Idris, Tanjong Malim 35900, Malaysia*

[2]*Nanotechnology Research Centre, Faculty of Science and Mathematics, Universiti Pendidikan Sultan Idris, Tanjong Malim 35900, Malaysia*

[3]*Tamhidi Centre, Universiti Sains Islam Malaysia, Bandar Baru Nilai, Nilai 71800, Malaysia*

[4]*School of Fundamental Science, Universiti Malaysia Terengganu, Kuala Terengganu 21030, Malaysia*

[5]*Department of Chemistry Education, Faculty of Mathematics and Natural Sciences, Yogyakarta State University, Yogyakarta 55281, Indonesia*

* ***Corresponding author:***

email: norain.sharif@fsmt.upsi.edu.my

Received: December 6, 2023
Accepted: January 12, 2024

DOI: 10.22146/ijc.91497

Abstract: *This study aims to enhance the targeted delivery of a powerful antioxidant, ferulate (FA), by developing a controlled release formulation (CRF) based on the incorporation of layered double hydroxide and Tween-80 polymeric surfactant. The layered double hydroxide-ferulate (LDH-FA) synthesized by co-precipitation method was homogenously mixed with the Tween-80 coater under continuous stirring. The successful Tween-80 coating was verified with PXRD analysis and supported by FTIR. No changes in interlayer distance between LDH-FA (at 17.4 and 8.7 Å) and LDH-FA-T80 (at 17.6 and 8.6 Å) were observed in the PXRD pattern. TGA/DTG analysis demonstrated good thermal stability of LDH-FA-T80, with the ability to withstand extreme temperatures up to 460 °C. The association of Tween-80 with LDH-FA progressively sustained the release time of FA in each aqueous solution, with a release time of up to 440 min. For both LDH-FA and LDH-FA-T80, the release of FA is through dissolution and anion exchange release mechanism (regulated by pseudo-second-order kinetic model). The study's findings suggest practical applications of FA in the pharmaceutical industry by implying the retarding effect triggered by Tween-80, offering new insights for the application of CRF to enhance the therapeutic effect of FA.*

Keywords: *controlled release formulation; layered double hydroxide; Tween-80, ferulate; intercalation*

■ INTRODUCTION

Layered double hydroxides (LDHs) are a type of layered materials that have garnered considerable interest to be employed as hosts for controlled release formulations (CRFs) due to their versatile composition, biocompatibility, low cytotoxicity, and ease synthesis technique. LDH consists of infinite sheets of positively charged brucite-type materials, but some of the divalent cations of the sheets have been substituted by tetrahedral cations in octahedral coordination [1-2]. The substitution triggers the formation of an excessive positive charge of LDH, which allows the numerous potential incorporations of intercalated anions in the interlayer gallery LDH. The general formula of LDH is $[M^{2+}_{(1-x)}\ L^{3+}_{x}\ (OH)_2]^{x+}A^{m-}_{x/m}{\cdot}nH_20$, where M^{2+} and L^{3+} represent divalent and trivalent metal cations, respectively, whereas A^{m-} stands for the guest ion [3].

In CRF systems, LDHs act as host materials that are

responsible for holding the drugs and sustaining the optimum release of drugs for a longer period. The sustained release of drugs promoted by CRF thereby contributes in improving the therapeutic efficacy of drugs [3-4]. Despite the amazing properties offered by LDHs, their low solubilization in water, agglomeration, and unsatisfactory targeted delivery have limited the potential of LDHs in CRF [5]. To deal with the aforementioned limitations, LDHs were attempted to be incorporated with a wide range of new materials, including polymeric surfactants [6-8]. Owing to the ability of polymeric surfactants to manipulate the nature of LDHs, predominantly in terms of size distribution, size of the particle, morphology, surface interaction, and zeta potential, this ability has therefore assisted in making LDHs more favorable for drug encapsulation [2,7-8].

The use of surfactants in pharmaceutical formulations was preferred because of their potential in improving drug solubility and inhibiting protein aggregation. Surfactants, which may exist in different forms of charges, either as non-ionic, anionic, cationic, or zwitterionic surfactants, act by lowering surface tension and modifying energy relationships at interfaces [9-10]. In the pharmaceutical industry, non-ionic surfactants (charge-free head groups) are used to encapsulate hydrophilic and hydrophobic drugs by forming emulsions, micelles, and niosomes [11]. The resemblance of nature between non-ionic surfactants and liposomes has made this surfactant an appropriate substitute for phospholipids. Rich phase separation behavior and low critical micellization temperature values owned by non-ionic surfactants are other critical features that befit them well for pharmaceutical purpose [12].

Polysorbates, also known as a tween, are synthetic non-ionic polymeric surfactants often used as stabilizers and emulsifiers in various pharmaceutical formulations [11-13]. Polysorbates comprise polyethoxy sorbitan fatty acid esters as the main components. The potential of LDH as a controlled release host material has been reported in previous studies [14-15]. However, to the best of our knowledge, no study has yet reported on the potential of incorporating polysorbate and LDH in improving the controlled release properties of ferulate. Therefore, throughout this study, we aimed to further explore the possibility of using Tween-80, polyoxyethylene-(20)-sorbitan monooleate, as a coating material to enhance the physicochemical stability, kinetics, and controlled release mechanism of the LDH-ferulate (LDH-FA) nanocomposite. The chemical structures of ferulate and Tween-80 are shown in Fig. 1 and 2, respectively.

The intercalated drug in the LDH-FA nanocomposite is ferulic acid, which is also known as 4-hydroxy-3-methoxycinnamic acid. It is commonly used as a strong autophagy enhancer for neurodegenerative disorders, skin antioxidants, and antibacterial wound dressing [16-18]. Ferulic acid's anti-inflammatory and antioxidant properties are also essential in maintaining the health of the digestive tract by protecting human intestinal epithelial cells [19]. To the best of our knowledge, no other literature has yet reported on the use of Tween-80 coating to improve the controlled release behavior of the LDH-FA nanocomposite.

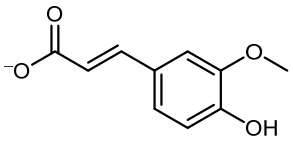

Fig 1. The chemical structure of ferulate

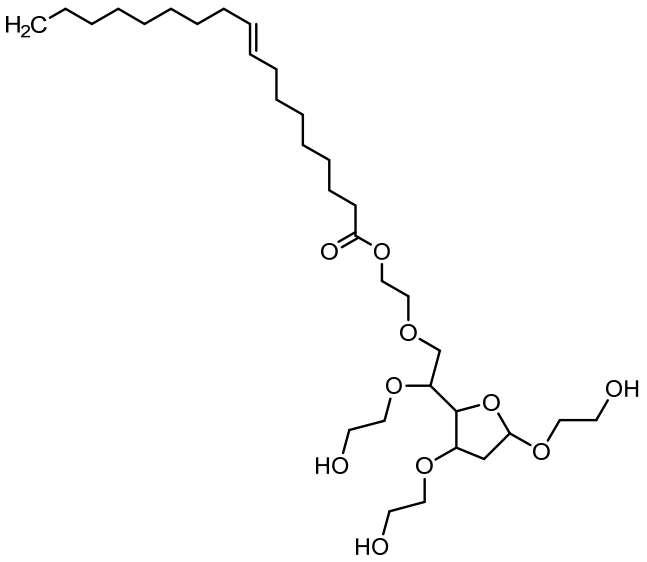

Fig 2. The chemical structure of Tween-80

■ EXPERIMENTAL SECTION

Materials

$Zn(NO_3)_2{\cdot}6H_2O$ (≥ 98% purity) and $Al(NO_3)_3{\cdot}9H_2O$ (≥ 98% purity) were purchased from Systerm. Ferulic acid (≥ 98% purity) and the coater Tween-80 were obtained from Acros Organics and Fisher Scientific, respectively. Methanol (≥ 99% purity) that was used to dissolve the ferulic acid was obtained from Systerm. The release media used in this study, aqueous sodium chloride, phosphate buffer saline (PBS) solution at pH 4.8 and 7.4, were purchased from Sigma-Aldrich. All reagents used in this study were used as received without further purification, and all aqueous solutions were prepared using deionized water.

Instrumentation

Several characterization techniques were carried out on the synthesized samples to determine their physicochemical properties. Powder X-ray diffraction (PXRD) analysis was carried out using a powder diffraction Bruker AXS with Cu Kα radiation (λ = 1.5406 Å). The PXRD analysis of all samples was conducted over the 2-theta range of 3–60°, with a scanning rate of 0.025° s^{-1}, at 60 kV and 60 mA. Fourier-transform infrared spectroscopy (FTIR) was conducted on a Thermo Nicolet 6700 Fourier transform infrared red. Spectra were collected over the range of 400–4000 cm^{-1}. TGA/DTG curves were obtained using a Perkin-Elmer Pyris 1 TGA Thermo Balance. Thermal analyses were performed in flowing argon gas from 25 to 1000 °C at a heating rate of 20 °C min^{-1}. The structural characterization of the samples was analyzed using field emission scanning electron microscopy (FESEM) for the morphology and transmission electron microscopy (TEM) for internal composition images. The morphologies of the samples were determined by FESEM at 5.0 kV and 10 k magnification. Both FESEM and TEM analyses were carried out using the same instrument model, which is a Hitachi model SU 8020 UHR. The CRF studies were conducted using a Lambda 25 Perkin Elmer ultraviolet-visible (UV-vis) spectrometer.

Procedure

Preparation of LDH-FA and LDH-FA-Tween 80 nanocomposite

The preparation of LDH-FA and LDH-FA-Tween 80 (LDH-FA-T80) involves multiple steps, which begin with the co-precipitation method to synthesize LDH. The LDH was synthesized using $Zn(NO_3)_2{\cdot}6H_2O$ and $Al(NO_3)_3{\cdot}9H_2O$, with a Zn/Al molar ratio, $R_{Zn/Al} = 3$. The resulting precipitated solid was stirred for 2 h under a nitrogen environment. The LDH-FA nanocomposite was prepared by intercalating 1.5 mmol FA into the interlamellar region of LDH using the ion exchange method. The synthesis method of the LDH and LDH-FA nanocomposite was reported in detail in our previous paper [20]. The loading percentage of FA in the LDH-FA nanocomposite intercalated using this method has been determined using elemental analysis, which is found to be 35.90% (w/w) and was reported in our previous study as well [20].

The LDH-FA-T80 nanocomposite was prepared using Tween-80 as a coater to encapsulate the synthesized LDH-FA nanocomposite. The Tween-80 coating procedure was initiated by preparing 100 mL of 0.25 M of the Tween-80 solution. The LDH-FA nanocomposite (0.1 g) was then added to the aqueous Tween-80 and magnetically stirred for 18 h at room temperature to allow the Tween-80 coating procedure to occur. The precipitates obtained from the coating procedure were centrifuged and dried in an oven overnight. The product collected was stored in a vial and denoted as LDH-FA-T80.

CRF and kinetic studies of the LDH-FA and LDH-FA-Tween-80-coated composite

Low-volume FA release for CRF studies were conducted using a UV-vis spectrometer, with deionized water, aqueous sodium chloride, and PBS as release media. Different pH pf PBS (pH = 4.8 and 7.4) were also set as one of the experimental parameters, so that the pH-dependency of the release behavior can be investigated as well. All release media were used at a

concentration of 0.1 mol L^{-1}, except for deionized water. The PBS solution was prepared by dissolving the PBS powder and diluted in a 1 L volumetric flask. The PBS solution was composed of 2.7 mM KCl, 137 mM NaCl and 1.76 mM K_2PO_4.

In this CRF study, LDH-FA (0.6 mg) was suspended in a cuvette containing 3.5 mL of release medium. The cuvette is covered with a cap and sealed with parafilm. The sealed cuvette was then analyzed using Lambda 25 Perkin Elmer UV-vis spectrometer. Similar UV-vis measurement setups were maintained for all samples in this study (UV-vis measurement setting: λ_{max} = 315 nm; time interval = 60 s; slit width = 1.0 nm; $ordinate_{max}$ = 1.0; $ordinate_{min}$ = 0.0). The cumulative FA release was measured until the absorbance curve from the UV-vis measurement reached a plateau, indicating that the diffusion equilibrium of FA was fully achieved. The absorbance readings obtained were then used to calculate the FA concentration using calibration curves of FA solutions generated from different concentrations of FA ranging from 25 to 250 µM. The data collected from the CRF studies will be used for the kinetic studies by fitting the data into zero order, first order, pseudo-second order, parabolic, and Fickian kinetic models.

■ RESULTS AND DISCUSSION

PXRD Analysis

The PXRD patterns of the LDH-FA, LDH, LDH-T80, and LDH-FA-T80 nanocomposites are depicted in Fig. 3. The PXRD patterns of the uncoated nanocomposite LDH-FA and the coated nanocomposite LDH-FA-T80 showed identical characteristic diffraction peaks to the LDH-FA nanocomposite at 2θ = 5°, 10°, 15°, 21°, and 26° with significant intensity diminishment. This revealed that Tween-80 may form on the surfaces of LDH and did not lead to a phase change, thereby demonstrating the success of the Tween-80 coating procedure on the interlamellar region of the LDH-FA nanocomposite [5,21].

The PXRD pattern demonstrated no expansion of the interlayer distance triggered by the Tween-80 coating procedure, as reflected by the comparable diffraction peaks of the LDH-FA and LDH-FA-T80 nanocomposites,

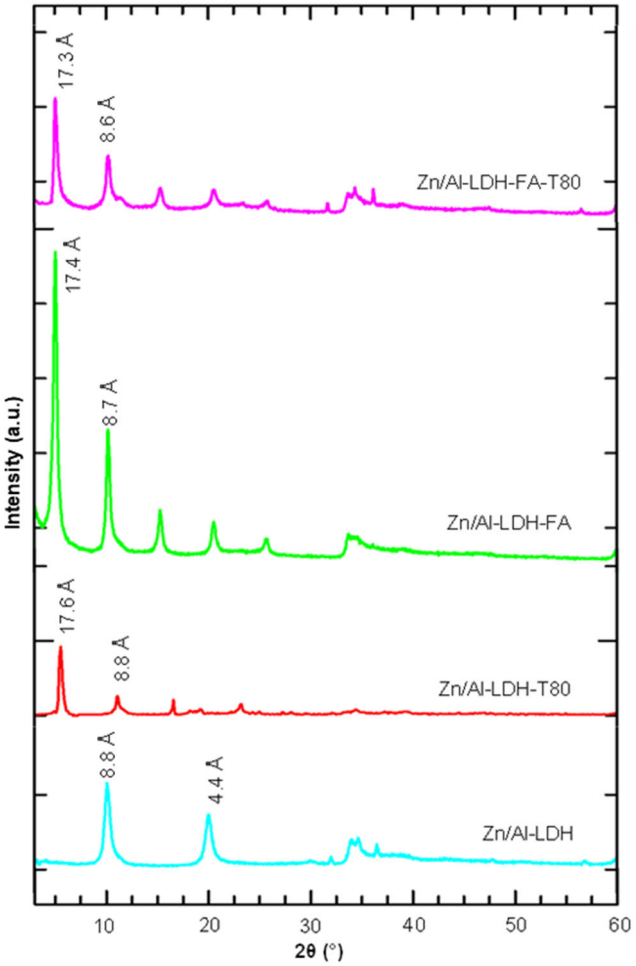

Fig 3. PXRD patterns of LDH-FA, LDH, LDH-T80, and LDH-FA-T80

thereby revealing two major revelations. Although LDH can be associated with polymer in many manners, such as exfoliation and intercalation, no expansion of interlayer distance after the coating procedure has revealed that the incorporation of LDH-FA with Tween-80 actually occurred via aggregation [5]. Unaffected interlayer distance also demonstrates that the presence of Tween-80 as the coating material did not cause any interference concerning the type of ions intercalated in the interlamellar region. Thus, signifies that the FA ions successfully remain intact in the interlamellar region of LDH-FA even after the coating procedure. The PXRD pattern generated proves that the LDH-FA can undergo the Tween-80 coating procedure without causing any disruption to the existing ions intercalated in their interlamellar region.

Spatial Orientation of Tween-80-Coated LDH-FA

The values of interlayer distance obtained from the PXRD analysis are also important for predicting the spatial orientation of the FA ion in the interlamellar region of LDH-FA. By deducting the value of the interlayer distance from the thickness of the LDH layer (4.8 Å), the height of the interlamellar region available to accommodate the intercalated FA ion can be calculated. Based on the height of the interlamellar region, Chemoffice software 2008 (Cambridge, MA) was used for spatial orientation prediction. Therefore, the comparison of the interlamellar region height of LDH-FA and LDH-FA-T80 allows the effect of Tween-80 coating on the spatial orientation of FA ions to be investigated. The proposed spatial orientation of LDH-FA and LDH-FA-T80 is illustrated in Fig. 4.

Based on the PXRD analysis, it was revealed that the interlayer distance of LDH-FA undergoes a slight reduction from 17.4 to 17.3 Å after this nanocomposite was coated with Tween-80. As illustrated in Fig. 4, the heights of the interlamellar regions of LDH-FA and LDH-FA-T80 were determined as 12.6 Å and 12.5 Å, respectively. The difference between the height of the interlamellar region is not much different; hence, this indicates that the spatial orientation is barely affected by the Tween-80 coating procedure. Before the coating procedure, the FA ion was held in the interlamellar region of LDH-FA in a monolayer orientation by electrostatic attraction, which exists between the COO^- part of the FA ion and the positively charged layer of LDH [20]. Minimal height reduction may, therefore, only cause the FA ion that accommodates the interlamellar region of LDH-FA-T80 to be slightly slanted than in LDH-FA. Hence, presume that the monolayer orientation of the intercalated FA ion in the interlamellar region of LDH-FA was preserved throughout the coating procedure. The interlayer distance in the PXRD diffraction peaks also elucidates the means by which the polymer was associated with the layered material, whether through intercalation, exfoliation, or aggregation [5]. Slight contraction of the interlayer distance in the PXRD diffraction peaks of LDH-FA-T80 has proven that Tween-80 interacts with LDH-FA by aggregation after the coating procedure [5,22]. The aggregation interactions between Tween-80 and LDH-FA are illustrated in the schematic diagram shown in Fig. 5.

FTIR Analysis

The results obtained from the FTIR analysis of LDH, Tween-80, LDH-T80, LDH-FA and LDH-FA-T80 are tabulated in Table 1 and depicted in Fig. S1. The absorption bands of methyl group (-CH_3) and -CH_2- stretching appear in the FTIR spectra of Tween-80, at 2925 and 2862 cm^{-1}, respectively. The absorption bands indicate the stretching vibrations of C=O (1738 cm^{-1}), C-O-C (1098 cm^{-1}) and –OH (3400 cm^{-1}). In the FTIR spectra of LDH, several absorption peaks appear, which reflect the stretching vibrations –OH (3450 cm^{-1}), symmetric stretching of nitrate (1385 and 1633 cm^{-1}), metal oxide stretching mode (600 cm^{-1}) and metal hydroxide stretching mode (430 cm^{-1}) [20]. Metal oxide

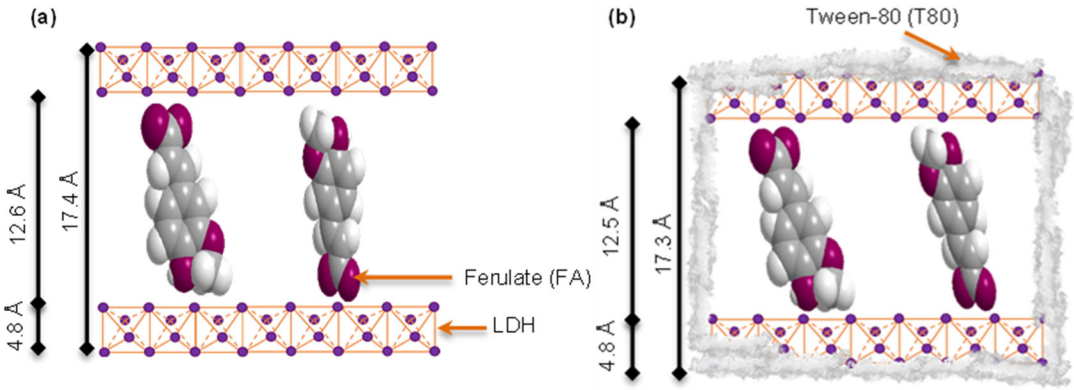

Fig 4. Spatial orientation of FA in the interlamellar region of LDH (a) before being coated with Tween-80 and (b) after being coated with Tween-80

Table 1. Data of FTIR analysis of Tween-80, LDH, LDH-T80, LDH-FA, and LDH-FA-T80

Characteristics	Wavenumber in each sample (cm^{-1})			
	LDH	Tween-80	LDH-T80	LDH-FA-T80
$-CH_3$	-	2925	2926	2925
$-CH_2-$	-	2862	2852	2855
C=O	-	1738	-	-
C–O–C	-	1098	1106	1032
–OH	3450	3400	3469	3455
NO_3^-	1385, 1633	-	-	-
M–O	600	-	607	613
M–OH	430	-	426	428

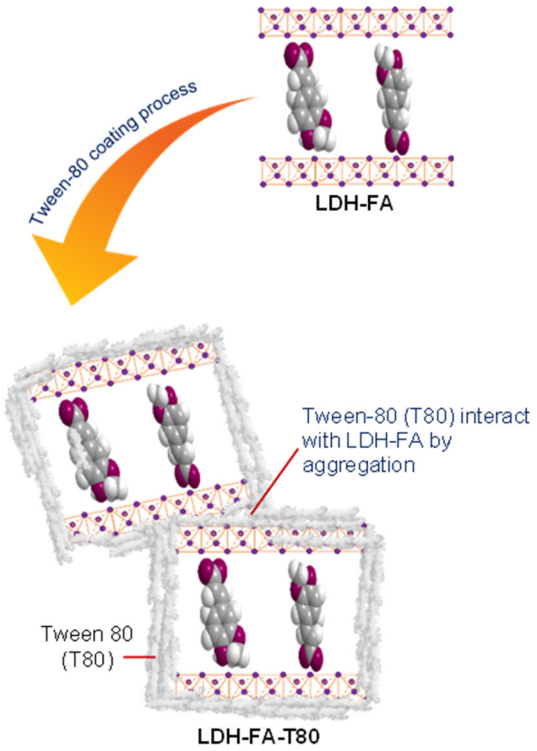

Fig 5. The aggregation interaction between Tween-80 and LDH-FA

stretching mode and metal hydroxide stretching mode were also found in the FTIR spectra of LDH-T80 at 607 and 426 cm^{-1}, as well as in the FTIR spectra of LDH-FA-T80 at 613 and 428 cm^{-1}, respectively.

The FTIR analysis also reveals that both LDH-T80 and LDH-FA-T80 nanocomposites have characteristic peaks of Tween-80, which supports the presence of Tween-80 on the surface of LDH and LDH-FA nanocomposite. The main functional groups of LDH-FA-T80 nanocomposite were $-CH_3$ at 2925 cm^{-1}, $-CH_2-$ at 2855 cm^{-1} and C–O–C at 1032 cm^{-1}. The same functional groups were found in LDH-T80 at 2926, 2852, and 1106 cm^{-1}, respectively. A broad band assigned to –OH stretching was found at 3455 and 3469 cm^{-1} for LDH-FA-T80 nanocomposite and LDH-T80, respectively. Nonetheless, the absorption band of C=O stretch was undetected in the LDH-FA-T80 nanocomposite and LDH-T80, probably because of the chemical interaction of Tween-80 with the surface of LDH via the oxygen of C=O group [23].

Thermal Stability Studies

The TGA analysis of LDH, Tween-80, LDH-FA, LDH-T80, and LDH-FA-T80 are shown in Fig. 6. In this section, the thermal degradation behavior of LDH-T80 and LDH-FA-T80 will be compared with their uncoated nanocomposite, LDH, and LDH-FA, respectively (Table 2). The thermal degradation of pure FA, LDH, and LDH-FA has been explained in detail in a previously published paper [20].

Founded on the results generated from the TGA analysis, the maximum temperature of the LDH-FA-T80 (460 °C) was found to be lower compared to the LDH-FA composite (663 °C). Even though there is a substantial reduction in their thermal stabilities, the ability of LDH-FA-T80 to be thermally stable up to 460 °C demonstrates the reliability of this nanocomposite to withstand extremely high temperatures.

In Fig. 6(b), the TGA analysis of Tween-80 demonstrates a dominant and intense peak at 413 °C, with a weight loss of 98.2% which denoted to the complete degradation of Tween-80. Fig. 6(d) shows that

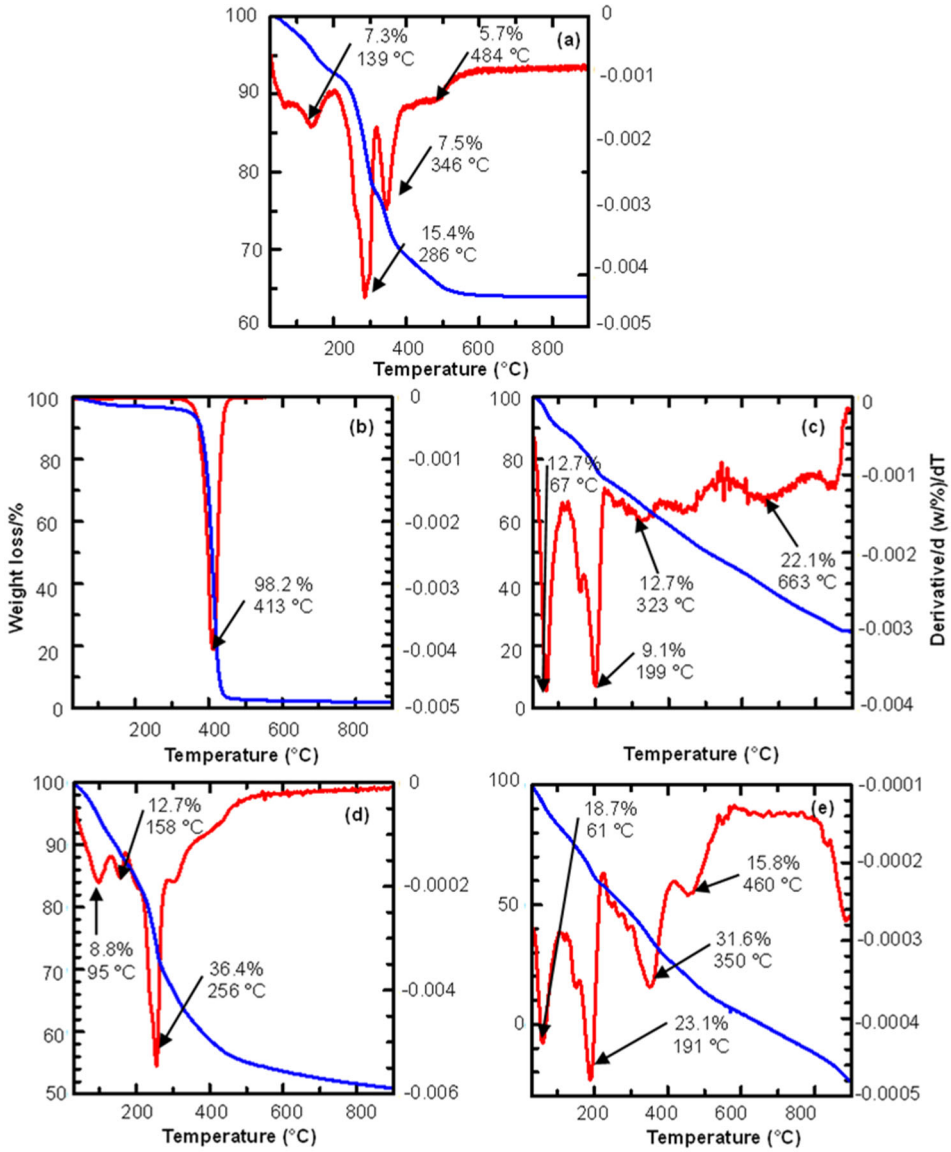

Fig 6. TGA/DTG curves of (a) LDH, (b) Tween-80, (c) LDH-FA, (d) LDH-T80, and (e) LDH-FA-T80

Table 2. Data of TGA analysis of Tween-80, LDH, LDH-T80, LDH-FA, and LDH-FA-T80

Thermal degradation		Samples				
		Tween-80	LDH	LDH-T80	LDH-FA	LDH-FA-T80
Stage 1	T_{max} (°C)	413	139.0	95.0	67.0	61.0
	Percentage (%)	98.2	7.3	8.8	12.7	18.7
Stage 2	T_{max} (°C)		286.0	158.0	199.0	191.0
	Percentage (%)		15.4	4.0	9.1	23.1
Stage 3	T_{max} (°C)		346.0	256.0	323.0	350
	Percentage (%)		7.5	36.4	12.7	31.6
Stage 4	T_{max} (°C)		484.0		663.0	460.0
	Percentage (%)		5.7		22.1	15.8
Ref.		Present paper	[20]	Present paper	[24]	Present paper

the thermal degradation of LDH-T80 progressed through three major stages at maximum temperatures of 95, 158, and 256 °C with weight losses of 8.8%, 12.7%, and 36.4%, respectively. The first stage occurred in the region around 100 °C, which is attributed to the water on the external surface of LDH and H_2O molecules within the interlamellar [24]. The second stage occurred in the region 150–200 °C, which corresponded to the degradation of Tween-80 surfactant [25]. The total weight loss of LDH-T80 was 49.2% compared to 35.9% for LDH, indicating that approximately 13.3% of Tween-80 was formed on the surface of LDH.

In Fig. 6(e), the TGA analysis of the LDH-FA-T80 nanocomposite shows four major stages with a total weight loss of 89.2%. The first stage happened around 61 °C with a weight loss of 18.7%, which resulted from the removal of H_2O molecules absorbed on the surface of LDH-FA-T80. The second stage occurred in the 120–220 °C region with a weight loss of 23.1% and can be related to the elimination of intercalated H_2O molecules as well as the degradation of surfactant [25, 26]. The third stage spanned the 220–420 °C region, with the largest weight loss (31.6%) due to dihydroxylation of the hydroxide layers. The fourth stage spanned 420–550 °C with a weight loss of 15.8%, which corresponded to the thermal degradation of organic species FA. Table 2 shows that the total weight loss of the LDH-FA-T80 nanocomposite is 89.2% compared to 70.8% for the LDH-FA nanocomposite, indicating that the LDH-FA nanocomposite was coated with 18.4% of Tween-80.

TEM Analysis

The TEM images of the LDH-FA and LDH-FA-T80 nanocomposite are illustrated in Fig. 7. After the coating procedure, the TEM micrographs of LDH-FA-T80 (Fig. 7(b)) showed a slight difference from the LDH-FA nanocomposite (Fig. 7(a)). As depicted in Fig. 7(b), the presence of LDH-FA-T80 as a dark center enclosed by a subtler shade of grey layer signifies that the surface of the LDH-FA nanocomposite was covered by Tween-80.

Surface Morphology Analysis

The surface morphologies of the LDH, LDH-FA LDH-Tween-80, and LDH-FA-T80 nanocomposite are illustrated in Fig. 8 FESEM images show different morphologies between uncoated LDH and LDH-FA nanocomposite when compared to their coated nanocomposites, LDH-T80 and LDH-FA-T80 nanocomposites. Slight surface transformation is noticeable after the coating procedure, as the typical non-uniform, irregular agglomerates of plate-like structures owned by the pristine LDH and LDH-FA nanocomposites appeared to flatten due to the presence of Tween-80. LDH-T80, and LDH-FA-T80 nanocomposites showed a smoother surface, and a stack of plate-like particles could not be clearly seen. These comparable data imply that the surfaces of the LDH and LDH-FA nanocomposite are successfully coated with Tween-80.

CRF Study of FA Release from the LDH-FA Nanocomposite

The release behavior of FA from both LDH-FA and LDH-FA-T80 was then studied in deionized water, aqueous sodium chloride (NaCl), and PBS (pH = 4.8 and 7.4) as the release media. Varying the type of release media used in this study allowed the influence of different ions to affect the release behavior of FA, whereas

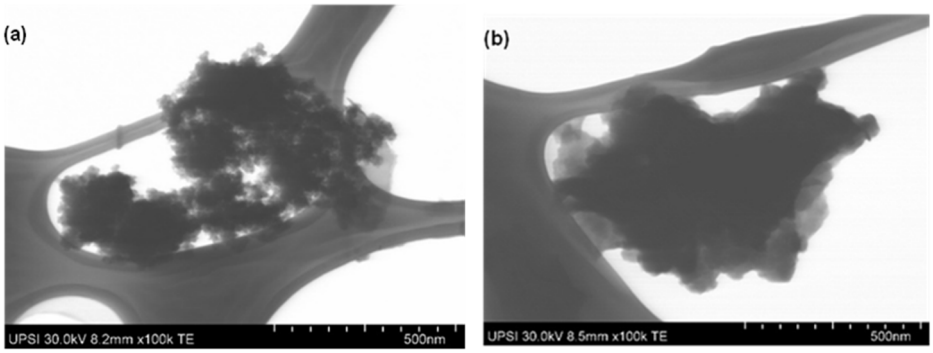

Fig 7. TEM images of (a) LDH-FA and (b) LDH-FA-T80 nanocomposites at 100 k magnification

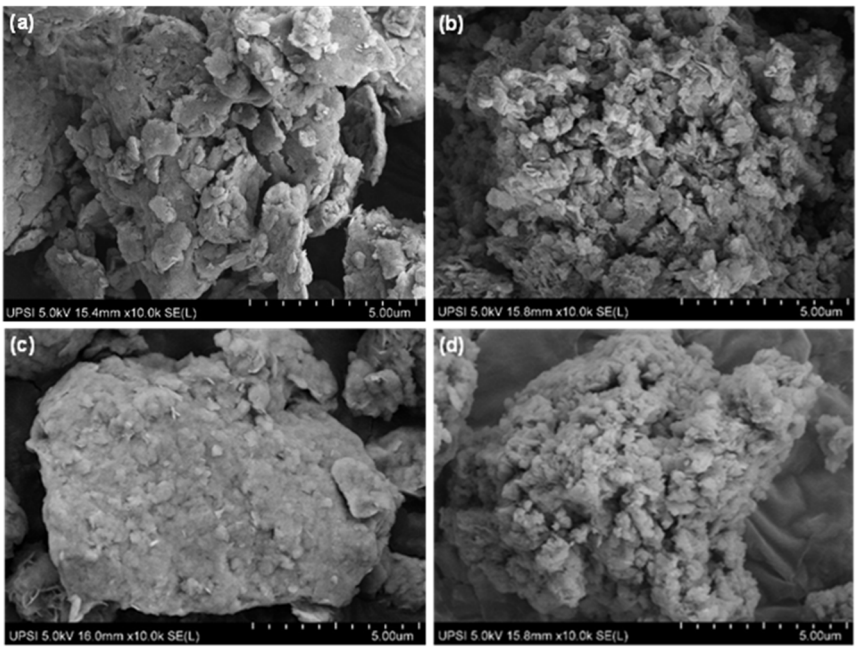

Fig 8. Surface morphology of (a) Tween-80, (b) LDH, (c) LDH-T80, (d) LDH-FA, and (e) LDH-FA-T80

different pH of PBS was used to investigate the release behavior of FA in terms of pH dependency. In this section, the cumulative amount of FA released was measured until the absorbance curve from the UV-vis measurement reached a plateau, indicating that the diffusion equilibrium of FA was fully achieved. The accumulated percentage release of FA from LDH-FA and LDH-FA-T80 were shown in Fig. 9 and tabulated in Table 3.

For the uncoated nanocomposite LDH-FA, the release of FA in deionized water was complete in almost 270 min (50.5% accumulated release of FA). In aqueous NaCl, a higher release rate of FA was observed, with a 280 min release time (64.8% accumulated release of FA). As for the release of FA from LDH-FA in PBS of pH 4.8 and 7.4, the absorbance curve from both UV-vis measurements reached a plateau at 220 min (76.9% accumulate release of FA) and 240 min (57.4% accumulate release of FA), respectively. The data collected in the CRF of FA from LDH-FA inferred that out of all release media, the rate of accumulation of FA from LDH-FA was the slowest when aqueous NaCl was used as release media. A higher release rate was observed as the release media were replaced with deionized water, and PBS (pH 4.8 and 7.4).

Different types of release media that were selected in this study, i.e., deionized water, aqueous NaCl, and PBS

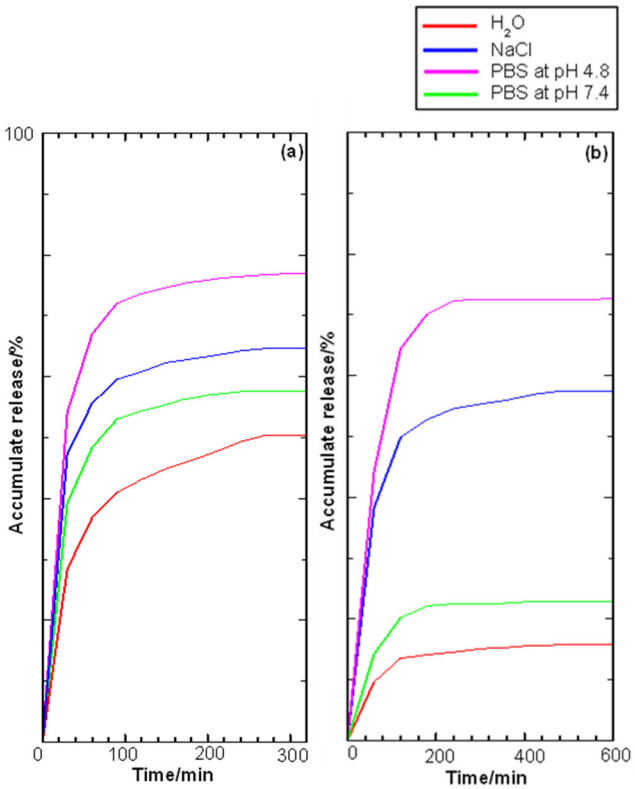

Fig 9. Release profiles of FA from (a) LDH-FA and (b) LDH-FA-T80 into various aqueous solutions

Table 3. Comparison of the accumulated percentage release of FA from LDH-FA and LDH-FA-T80 into aqueous solutions of deionized water, NaCl, and PBS (pH 4.8 and 7.4)

Aqueous solutions	LDH-FA		LDH-FA-T80	
	Percentage release (%)	Release time (min)	Percentage release (%)	Release time (min)
H_2O	50.5	270	17.2	440
NaCl	64.8	280	59.5	480
PBS (pH 4.8)	76.9	220	72.7	300
PBS (pH 7.4)	57.4	240	22.3	400

solutions, will supply different types of anions during the controlled release study, which are OH^-, Cl^-, and PO_4^{3-} anions, respectively. Considering LDH is a type of host layered material with great ion exchange ability, and the anions supplied by the release media have smaller radii, higher affinity, and greater charge density compared to the intercalated FA, exposing LDH-FA and LDH-FA-T80 nanocomposites in these release media will, thereby, lead to the occurrence of anion exchange between the intercalated FA anions and the anions present in the release media. Different properties of the anions in the release media, particularly in terms of affinity, size, and charge density, will influence the release behavior of FA, as reflected by the varied accumulated percentage release and release time, as shown in the release profile (Fig. 9).

Based on the data obtained in the release study, the slowest release of FA occurs when aqueous NaCl is used as the release medium. Slower rate of the anion exchange process can be related to the nature of Cl^- anion, which existed as simple monoatomic and monovalent ions with lower charge density, compared to OH^- and PO_4^{3-}. Due to this reason, Cl^- will have a lower affinity towards the positively charged layer of LDH, thereby undergoing an anion exchange process in a slower manner than the polyatomic OH^- and PO_4^{3-} anions. A recent study has reported that LDH tends to have higher selectivity towards OH^- than Cl^- [27]. The order of anion selectivity can be arranged according to their affinity toward LDH, in the sequence of $CO_3^{2-} > OH^- > F^- > Cl^- > Br^- > NO_3^-$, with CO_3^{2-} being the most preferable anions by LDH [28]. The slowest release rate of FA in aqueous solution containing Cl^-, is indeed in good agreement with many release studies related to controlled release formulation [29-31].

In this section, the dependency of the FA release rate on the pH of the aqueous solution was also studied using a PBS solution of different pH. The manipulated pH values in the study, pH 4.8 and 7.4, were selected to simulate acidic and basic environments so that the impact of the acidity or basicity of the aqueous solution on the release behavior of FA can be thoroughly investigated. Based on the release profile shown in Fig. 9, noticeable differences between the release behavior of FA in PBS solution at pH 4.8 and 7.4 were observed. The release rate of FA in PBS solution at pH 4.8 demonstrated a faster release process, with a higher percentage of accumulated release compared with the release of FA in PBS solution at pH 7.4. These findings can be related to different release mechanisms of FA from LDH-FA, resulting from different degrees of stability of LDH hold when exposed to acidic or basic release media.

LDHs are generally made up of positively charged metal hydroxide layers that are balanced by negatively charged anions and water molecules positioned in the interlamellar region [32]. The hydroxide layer found in LDHs is unstable in acidic environments; therefore, it tends to dissolve and release the anions that were intercalated in their interlamellar region through the disintegration of the hydroxide layer and anion exchange process [33]. The instability of the hydroxide layer of LDH in an acidic environment weakens the electrostatic attraction that holds FA in their interlamellar region, making it easier for the FA to be exchanged with PO_4^{3-} anion supplied by the PBS solution at pH 4.8. The highest percentage of accumulated release and fastest release rate of FA when using PBS solution at pH 4.8 as release media, as shown

in Fig. 9, has thereby supported the proposed release mechanism. As for the release of FA in PBS solution at pH 7.4, a slower release of FA can be observed from the release profile, particularly because the hydroxide layer is more stable in the basic environment. Hence, only allow the release process to occur via ion exchange [33]. Therefore, these results evidently show that the release behavior of FA from LDH-FA hinges on the pH of the release environment. The high structural stability of LDHs in the high alkaline range is also in good agreement with a previous study [27].

As for the release of FA from the Tween-80-coated nanocomposite LDH-FA-T80, the absorbance curve from both UV-vis measurements reached a plateau in almost 480 min release time (59.5% accumulated release of FA) in aqueous NaCl, 440 min (17.2% accumulated release of FA) in deionized water, 400 min (22.3% accumulate release of FA) in PBS of pH 7.4 and 300 min (72.7% accumulate release of FA) in PBS of pH 4.8. Therefore, the CRF data of FA from both LDH-FA and LDH-FA-T80 revealed a similar trend of release behavior. The release of FA from both LDH-FA and LDH-FA-T80 occurred faster during the early phase of the release process and became slower before reaching equilibrium at their maximum accumulated release. The slowest release rate was recorded when aqueous NaCl was used, followed by PBS of pH 7.4, deionized water and PBS of pH 4.8.

Comparatively, the release behavior of FA from both LDH-FA and LDH-FA-T80 showed similar trends. However, the release time of FA was further prolonged with the presence of Tween 80 as the coater. The Tween-80 coating leads to a more progressive release, as demonstrated by the slower release rate of FA in all release media, particularly in aqueous NaCl, with the release time extended from 280 to 480 min. When considering the controlled release effect instigated by the presence of Tween-80, the prolonged release behavior is possibly related to the retarding effect triggered by the encapsulation effect of Tween-80 on LDH-FA [34]. Therefore, the prolonged effect demonstrated by the release data has shown the potential of using Tween-80 coater as a promising material in enhancing the controlled release behavior of targeted substances.

Kinetic Study of LDH-FA and LDH-FA-T80 Nanocomposites Released into Various Aqueous Solutions

Mathematical modeling is a significant approach to interpreting the release mechanism of a substance by providing information on its delivery manner, mass transfer and kinetics. Therefore, in this section, the in vitro release study data obtained were fitted to several kinetic models to gain a deeper understanding of the release mechanism of FA from both LDH-FA and LDH-FA-T80 nanocomposites. The kinetic models selected to fit the release data collected were zeroth-order (Eq. (1)) [35], first-order (Eq. (2)) [36], pseudo-second-order (Eq. (3)) [37], parabolic diffusion (Eq. (4)) [38] and Fickian diffusion (Eq. (5)) [39],

$$x = t + c \tag{1}$$

$$-\log\left(1 - \frac{M_i}{M_f}\right) = t + c \tag{2}$$

$$\frac{t}{Mi} = \frac{1}{M^2{}_f} + \frac{t}{M_f} \tag{3}$$

$$\frac{M_i}{M_f} = kt^{0.5} + c \tag{4}$$

$$\frac{M_i}{M_f} = kt^n \tag{5}$$

where x, accumulated percentage release of FA anions at time t, M_i is the amount of FA at the beginning of the release process, M_f is the cumulative amount of FA released when the release process is completed, n is an empirical parameter for the release mechanism, and c is a constant value for the related equations.

Using the equations of the aforementioned kinetic models, the correlation coefficients, r^2, rate constant, k, and half-time for the release process, $t_{1/2}$, can be determined. $t_{1/2}$ refers to the duration for LDH-FA and LDH-FA-T80 to reach half of the maximum accumulated percentage release of FA during the controlled release study. The best fit of the data to these five kinetic models was evaluated on the basis of the comparisons of r^2 values of all kinetic models. A kinetic model with r^2 nearest value of 1.00 will be deemed as the most appropriate fit kinetic model.

The kinetic simulation for the release data of FA from LDH-FA using various kinetic models, shown in

Fig. 10, reveals that the linearization of kinetic models seems to be the most ideal when the data are represented using a pseudo-second-order kinetic model. The kinetic data obtained for the release data of FA from LDH-FA is tabulated in Table 4. The r^2 values for the data fitted into this model were found to lie in the range of 0.994–0.999, thereby implying that the dissolution and anion exchange processes are mainly responsible for the release mechanism of FA from LDH-FA.

The dissolution mechanism of LDHs was described to occur in two stages, in which rapid formation of surface reactive sites by –OH protonation takes place in the first stage, whereas the second stage involves gradual disengagement of metal cation [40]. Considering that the release of FA involves an anionic exchange mechanism, the intercalated FA anion must, therefore leave the interlamellar region of LDH-FA and migrate to the release media so that the unbalanced

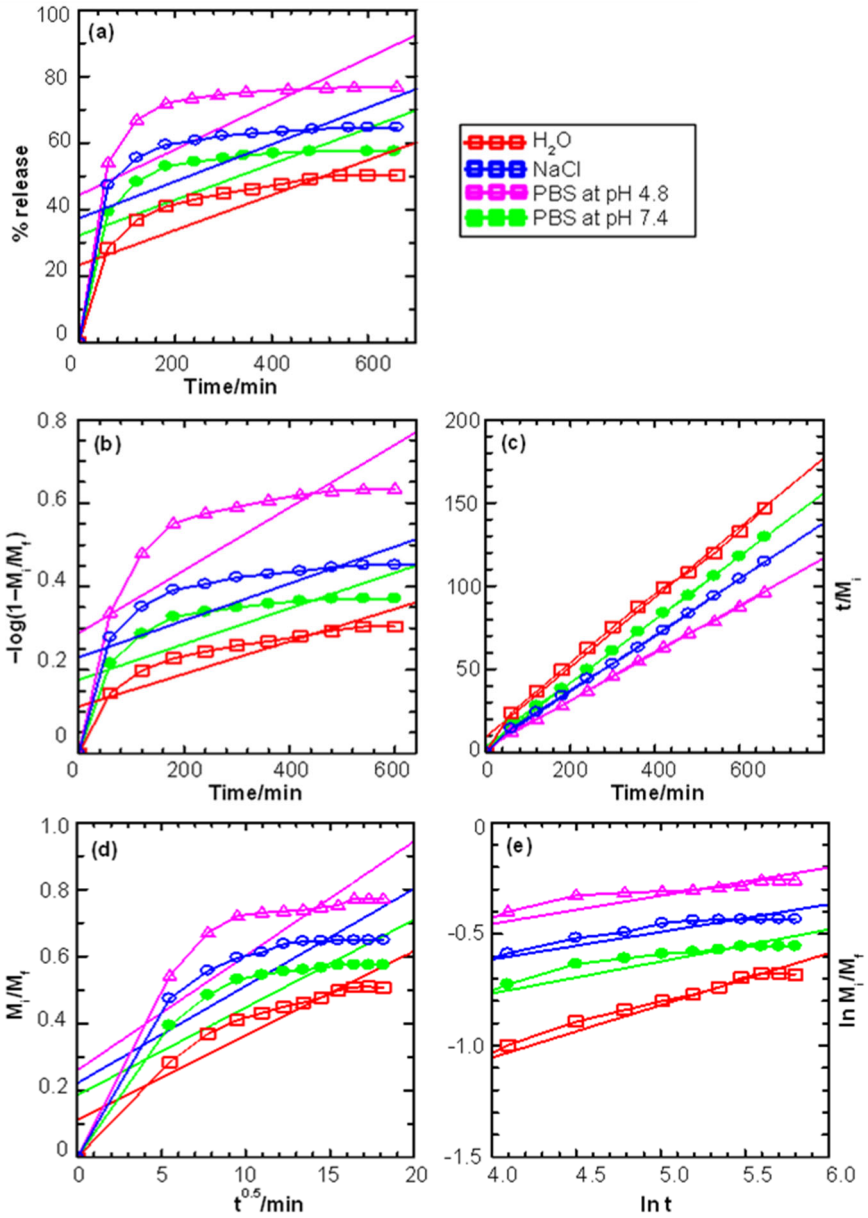

Fig 10. Fitting of the data for FA release from LDH-FA into various aqueous solutions for the (a) zeroth-order, (b) first-order, (c) pseudo-second-order, (d) parabolic diffusion, and (e) Fickian diffusion models

Table 4. Comparison of rate constants (k), regression values (r^2), and half-life ($t_{1/2}$) obtained from the fitting of the release data from LDH-FA into aqueous solutions of deionized water, NaCl, PBS at pH 4.8, and 7.4

Aqueous solution	Zeroth-order	First-order	Parabolic diffusion	Fickian diffusion	Pseudo-second-order		
	r^2	r^2	r^2	r^2	r^2	k ($\times10^{-2}s^{-1}$)	$t_{1/2}$ (min)
H_2O	0.634	0.739	0.871	0.964	0.994	1.867	26.500
NaCl	0.626	0.550	0.711	0.886	0.999	4.246	20.300
PBS (pH 4.8)	0.425	0.607	0.711	0.842	0.999	3.208	21.500
PBS (pH 7.4)	0.454	0.582	0.734	0.863	0.999	4.054	22.200

charge caused by the migration of FA can be counterbalanced by the incoming anion supplied by the release media.

The results obtained also show that the $t_{1/2}$ calculated for the release of FA in PBS at pH 4.8 (21.5 min) is less than the $t_{1/2}$ for the release of FA in PBS at pH 7.4 (22.2 min). These results indicate that the release of FA occurs faster in a medium with higher acidity. The dissolution behavior of LDH in a mildly acidic environment (PBS at pH 4.8) is governed by the equilibrium achieved between the particle surface reactive sites and the dissolved species. Therefore, the dependence of the reaction rate on pH demonstrated in this study is in good agreement with those reported in a previous study [40].

As for the release of FA from LDH-FA-T80, it was found that the pseudo-second-order model also demonstrated a better satisfactory release kinetic process of FA from LDH-FA-T80 compared with the other kinetic models (Fig. 11). The plot of t/M_t vs. t for the release of FA from LDH-FA-T80 in Fig. 11(c) shows that fair straight lines were generated through the fitting. With the simulation of the release data of FA from LDH-FA-T80 into all kinetic models used in the study, the r^2 values of release data fitting with pseudo-second-order model are in the range of 0.997–0.998, while the other kinetic models are in the range of 0.460–0.844 (Table 5). Therefore, this indicates that the release mechanism of FA, which is through dissolution and anion exchange release mechanism, was maintained despite Tween-80

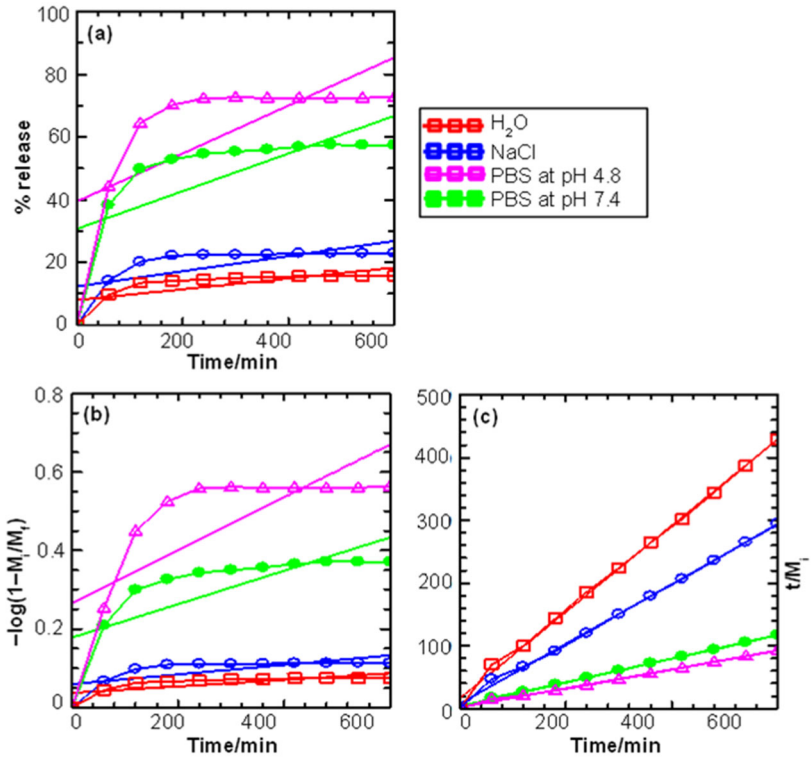

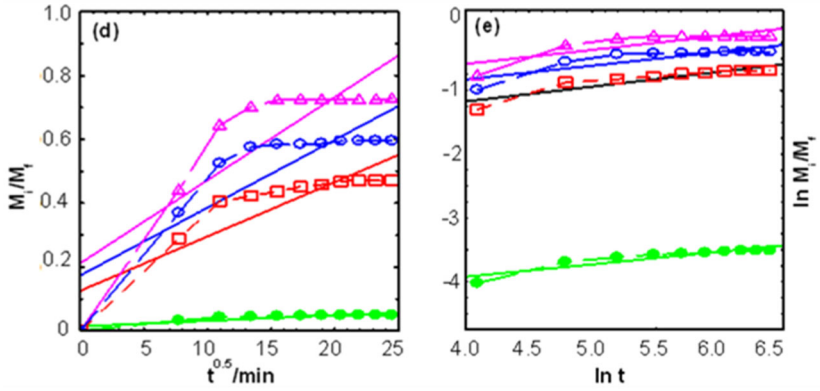

Fig 11. Fitting of the data for FA release from LDH-FA-T80 into various aqueous solutions for the (a) zeroth-order, (b) first-order, (c) pseudo-second-order, (d) parabolic diffusion, and (e) Fickian diffusion models

Table 5. Comparison of rate constants (k), regression values (r^2), and half-life ($t_{1/2}$) obtained from fitting the release data from LDH-FA-T80 into aqueous solutions of deionized water, NaCl, PBS at pH 4.8, and 7.4

Aqueous solution	Zeroth-order	First-order	Parabolic diffusion	Fickian diffusion	Pseudo-second-order		
	r^2	r^2	r^2	r^2	r^2	k ($\times10^{-1}s^{-1}$)	$t_{1/2}$ (min)
H_2O	0.525	0.541	0.791	0.836	0.997	1.168	41.600
NaCl	0.460	0.488	0.745	0.727	0.998	1.114	48.600
PBS (pH 4.8)	0.464	0.548	0.739	0.699	0.997	0.381	45.300
PBS (pH 7.4)	0.488	0.572	0.760	0.844	0.998	0.400	50.000

being present as a coater for the nanocomposite.

Even though the release behavior of FA from both systems (LDH-FA and LDH-FA-T80) shared the same release mechanisms (as indicated by the pseudo-second-order kinetic model governed by these nanocomposites), a significant difference in terms of their $t_{1/2}$ can be clearly observed from the kinetic data tabulated in Table 4 and 5. The $t_{1/2}$ for the release data of FA in LDH-FA is in the range of 20.3–26.5 s, whereas for the release data of FA in LDH-FA-T80, the $t_{1/2}$ lies in the range of 41.6–50.0 s. The potential of Tween-80 in prolonging the release process can be correlated with the nature of Tween-80. Tween-80 is an amphiphilic substance with both hydrophilic and hydrophobic moieties in the same molecule [41]. The backbone structure of Tween-80 is a sorbitan ring with poly(ethylene oxide) conjugated to hydroxyl groups (hydrophilic region) and oleate fatty acid ester (hydrophobic region) associated with the polyoxyethylene sorbitan portion of the molecule. The amphiphilic nature of Tween-80 permits it to self-assemble into micelles in aqueous solutions after reaching critical micellar concentrations. The hydrophilic region of Tween-80 is responsible for keeping the micelles stable and decreasing undesirable FA interactions with the outer medium, thereby protecting the nanocomposite and promoting slower and sustained release of FA. The presence of Tween-80 was also expected to facilitate the targeted delivery of FA by increasing their bioavailability. Recent studies have reported the potential of micelle formation to increase the permeability of drugs across biological membranes and enhance the aqueous solubility of hydrophobic drugs *in vivo* and *in vitro* [12,42]. The results obtained in the present work confirm that the formation of Tween-80 micelles is an effective platform for achieving efficient and targeted delivery of FA.

■ CONCLUSION

This study highlights the potential of Tween-80 polymeric surfactant in enhancing the controlled release formulation for the delivery of FA. The LDH-FA-T80 nanocomposite was prepared for loading and controlling the release of FA using LDH and Tween-80 as the host and coating materials, respectively. The

synthesized LDH-FA-T80 was characterized by PXRD, FTIR, TGA/DTG, TEM, and FESEM to verify the success of the coating procedure and to investigate its physicochemical properties. The results generated from the characterization study revealed the success of the coating procedure, and the intercalated FA was preserved in the interlamellar region of LDH-FA-T80. The LDH-FA-T80 also exhibited excellent thermal stability. The release profile obtained reveals the potential of Tween-80 in CRF, reflected by the significantly prolonged release time of FA from LDH-FA-T80. The release of FA from LDH-FA-T80 was also found to be influenced by the presence of the anions in the release media and pH dependence. The release process of FA from the LDH-FA-T80 nanocomposite can be well described by pseudo-second-order release kinetics, which signifies the dissolution and anion exchange process. The retarding effect triggered by Tween-80 promotes the sustained release of FA, thereby demonstrating its potential in the pharmaceutical industry.

■ ACKNOWLEDGMENTS

The authors wish to thank Universiti Pendidikan Sultan Idris and Ministry of Education Malaysia for their support during completing the research. This work was supported by the Fundamental University Research Grant (GPUF) Grant No. 2021–0205–103–01.

■ CONFLICT OF INTEREST

None declared.

■ AUTHOR CONTRIBUTIONS

Sharifah Norain Mohd Sharif: Conceptualization, Methodology, Data curation, Writing- Original draft preparation and Funding acquisition. Norhayati Hashim: Conceptualization, Writing- Reviewing and Editing. Illyas Md Isa: Conceptualization, Methodology. Maizatul Najwa Jajuli: Conceptualization, Data curation. Afif Arifin: Conceptualization, Writing- Reviewing and Editing. Norlaili Abu Bakar: Writing- Reviewing and Editing, Project administration. Mazidah Mamat: Data curation, Writing- Reviewing and Editing. Suyanta: Conceptualization, Methodology. All authors agreed to the final version of this manuscript.

■ REFERENCES

[1] Sheikh Mohd Ghazali, S.A.I., Sarijo, S.H., and Hussein, M.Z., 2021, New synthesis of binate herbicide-interleaved anionic clay material: Synthesis, characterization and simultaneous controlled-release properties, *J. Porous Mater.*, 28 (2), 495–505.

[2] Peralta, M.F., Mendieta, S.N., Scolari, I.R., Granero, G. E., and Crivello, M. E., 2021, Synthesis and release behavior of layered double hydroxides–carbamazepine composites, *Sci. Rep.*, 11 (1), 20585.

[3] Rad, S., and Yazdi, E., 2021, Study of nano-dual organic-hydroxide drug delivery system for anticancer drugs, *Medbiotech J.*, 5 (1), 22–27.

[4] Mohiuddin, I., Grover, A., Aulakh, J.S., Malik, A.K., Lee, S.S., Brown, R.J.C., and Kim, K.H., 2021, Starch-Mg/Al layered double hydroxide composites as an efficient solid phase extraction sorbent for non-steroidal anti-inflammatory drugs as environmental pollutants, *J. Hazard. Mater.*, 401, 123782.

[5] Kura, A.U., Hussein-Al-Ali, S.H., Hussein, M.Z., and Fakurazi, S., 2014, Preparation of Tween 80-Zn/Al-levodopa-layered double hydroxides nanocomposite for drug delivery system, *Sci. World J.*, 2014, 104246.

[6] Barkhordari, S., and Alizadeh, A., 2022, Fabrication of pH-sensitive chitosan/layered double hydroxide (LDH)/Fe_3O_4 nanocomposite hydrogel beads for controlled release of diclofenac, *Polym. Bull.*, 79 (7), 5533–5548.

[7] Liu, Z., Lansley, A.B., Duong, T.N., Smart, J.D., and Pannala, A.S., 2022, Increasing cellular uptake and permeation of curcumin using a novel polymer-surfactant formulation, *Biomolecules*, 12 (12), 1739.

[8] Constantino, V.R.L., Figueiredo, M.P., Magri, V.R., Eulálio, D., Cunha, V.R.R., Alcântara, A.C.S., and Perotti, G.F., 2023, Biomaterials based on organic polymers and layered double hydroxides nanocomposites: Drug delivery and tissue engineering, *Pharmaceutics*, 15 (2), 413.

[9] Bozorgian, A., Aboosadi, Z.A., Mohammadi, A., Honarvar, B., and Azimi, A., 2020, Determination of CO_2 gas hydrates surface tension in the presence

of non-ionic surfactants and TBAC, *Rev. Roum. Chim.*, 65 (12), 1061–1065.

[10] Baek, S., Shin, D., Kim, G., Lee, A., Noh, J., Choi, B., Huh, S., Jeong, H., and Sung, Y., 2021, Influence of amphoteric and anionic surfactants on stability, surface tension, and thermal conductivity of Al_2O_3/water nanofluids, *Case Stud. Therm. Eng.*, 25, 100995.

[11] Mandal, S., Banerjee, C., Ghosh, S., Kuchlyan, J., and Sarkar, N., 2013, Modulation of the photophysical properties of curcumin in non-ionic surfactant (Tween-20) forming micelles and niosomes: A comparative study of different microenvironments, *J. Phys. Chem. B*, 117 (23), 6957–6968.

[12] Ravichandran, V., Lee, M., Nguyen Cao, T.G., and Shim, M.S., 2021, Polysorbate-based drug formulations for brain-targeted drug delivery and anticancer therapy, *Appl. Sci.*, 11 (19), 9336.

[13] Nilsson, E.J., Lind, T.K., Scherer, D., Skansberger, T., Mortensen, K., Engblom, J., and Kocherbitov, V., 2020, Mechanisms of crystallisation in polysorbates and sorbitan esters, *CrystEngComm*, 22 (22), 3840–3853.

[14] Lima, E., Flores, J., Cruz, A.S., Leyva-Gómez, G., and Krötzsch, E., 2013, Controlled release of ferulic acid from a hybrid hydrotalcite and its application as an antioxidant for human fibroblasts, *Microporous Mesoporous Mater.*, 181, 1–7.

[15] Sousa, R., da Silva, B.J.M., Dias, A.A., Meneses, C.C.F., Bentes, B.A., Silva, E.O., Remédios, C.M.R., Feio, W.P., Masson, O., Alves, C.N., Arruda, M.M.S.P., and Lameira, J., 2019, Ferulate anion intercalated into Zn/Al layered double hydroxide: A promising intercalation compound for inhibition of *Leishmania (L.) amazonensis*, *J. Braz. Chem. Soc.*, 30 (6), 1178–1188.

[16] Long, T., Wu, Q., Wei, J., Tang, Y., He, Y.N., He, C.L., Chen, X., Yu, L., Yu, C.L., Law, B.Y.K., Wu, J.M., Qin, D.L., Wu, A.G., and Zhou, X.G., 2022, Ferulic acid exerts neuroprotective effects via autophagy induction in *C. elegans* and cellular models of Parkinson's disease, *Oxid. Med. Cell. Longevity*, 2022, 372567.

[17] Sivakumar, S., Murali, R., Arathanaikotti, D., Gopinath, A., Senthilkumar, C., Kesavan, S., and Madhan, B., 2021, Ferulic acid loaded microspheres reinforced in 3D hybrid scaffold for antimicrobial wound dressing, *Int. J. Biol. Macromol.*, 177, 463–473.

[18] Mancuso, A., Cristiano, M.C., Pandolfo, R., Greco, M., Fresta, M., and Paolino, D., 2021, Improvement of ferulic acid antioxidant activity by multiple emulsions: *In vitro* and *in vivo* evaluation, *Nanomaterials*, 11 (2), 425.

[19] Hwang, H.J., Lee, S.R., Yoon, J.G., Moon, H.R., Zhang, J., Park, E., Yoon, S.I., and Cho, J.A., 2022, Ferulic acid as a protective antioxidant of human intestinal epithelial cells, *Antioxidants*, 11 (8), 1448.

[20] Muda, Z., Hashim, N., Isa, I., and Ali, N.M., 2016, Preparation of layered material Zn/Al-layered double hydroxide-ferulate nanocomposites, *Sainmatika*, 13 (2), 35–47.

[21] Javid, A., Ahmadian, S., Saboury, A.A., Kalantar, S.M., and Rezaei-Zarchi, S., 2014, Novel biodegradable heparin-coated nanocomposite system for targeted drug delivery, *RSC Adv.*, 4 (26), 13719–13728.

[22] Sharif, S.N.M., Hashim, N., Isa, I.M., Bakar, S.A., Saidin, M.I., Ahmad, M.S., Mamat, M., Hussein, M.Z., and Zainul, R., 2021, Polymeric nanocomposite-based herbicide of carboxymethyl cellulose coated-zinc/aluminium layered double hydroxide-quinclorac: A controlled release purpose for agrochemicals, *J. Polym. Environ.*, 29 (6), 1817–1834.

[23] Khan, Y., Durrani, S.K., Siddique, M., and Mehmood, M., 2011, Hydrothermal synthesis of alpha Fe_2O_3 nanoparticles capped by Tween-80, *Mater. Lett.*, 65 (14), 2224–2227.

[24] Dong, L., Gou, G., and Jiao, L., 2013, Characterization of a dextran–coated layered double hydroxide acetylsalicylic acid delivery system and its pharmacokinetics in rabbit, *Acta Pharm. Sin. B*, 3 (6), 400–407.

[25] Castro, D.C., Cavalcante, R.P., Jorge, J., Martines, M.A.U., Oliveira, L.C.S., Casagrande, G.A., and Machulek Jr., A., 2016, Synthesis and

characterization of mesoporous Nb_2O_5 and its application for photocatalytic degradation of the herbicide methylviologen, *J. Braz. Chem. Soc.*, 27 (2), 303–313.

[26] Wei, M., Guo, J., Shi, Z., Yuan, Q., Pu, M., Rao, G., and Duan, X., 2007, Preparation and characterization of L-cystine and L-cysteine intercalated layered double hydroxides, *J. Mater. Sci.*, 42 (8), 2684–2689.

[27] Mir, Z.M., Gomes, C., Bastos, A.C., Sampaio, R., Maia, F., Rocha, C., Tedim, J., Höche, D., Ferreira, M.G.S., and Zheludkevich, M.L., 2021, The stability and chloride entrapping capacity of ZnAl-NO_2 LDH in high-alkaline/cementitious environment, *Corros. Mater. Degrad.*, 2 (1), 78–99.

[28] Costa, D.G., Rocha, A.B., Souza, W.F., Chiaro, S.S.X., and Leitão, A.A., 2012, Comparative structural, thermodynamic and electronic analyses of ZnAlA^{n-} hydrotalcite-like compounds (A^{n-}=Cl^-, F^-, Br^-, OH^-, CO_3^{2-} or NO_3^-): An *ab initio* study, *Appl. Clay Sci.*, 56, 16–22.

[29] Sheikh Mohd Ghazali, S.A.I., Hussein, M.Z., and Sarijo, S.H., 2013, 3,4-Dichlorophenoxyacetate interleaved into anionic clay for controlled release formulation of a new environmentally friendly agrochemical, *Nanoscale Res. Lett.*, 8 (1), 362.

[30] Li, S., Shen, Y., Xiao, M., Liu, D., and Fan, L., 2015, Synthesis and controlled release properties of β-naphthoxyacetic acid intercalated Mg–Al layered double hydroxides nanohybrids, *Arabian J. Chem.*, 12 (8), 2563–2571.

[31] Sarijo, S.H., Sheikh Mohd Ghazali, S.A.I., Hussein, M.Z., and Ahmad, A.H., 2015, Intercalation, physicochemical and controlled release studies of organic-inorganic–herbicide (2,4,5-tricholorphenoxy butyric acid) nanohybrid into hydrotalcite-like compounds, *Mater. Today: Proc.*, 2 (1), 345–354.

[32] Sajid, M., Sajid Jillani, S.M., Baig, N., and Alhooshani, K., 2022, Layered double hydroxide-modified membranes for water treatment: Recent advances and prospects, *Chemosphere*, 287, 132140.

[33] Abniki, M., Moghimi, A., and Azizinejad, F., 2021, Synthesis of calcium-layered double hydroxide based nanohybrid for controlled release of an anti-inflammatory drug, *J. Chin. Chem. Soc.*, 68 (2), 343–352.

[34] Kameshima, Y., Sasaki, H., Isobe, T., Nakajima, A., and Okada, K., 2009, Synthesis of composites of sodium oleate/Mg-Al-ascorbic acid-layered double hydroxides for drug delivery applications, *Int. J. Pharm.*, 381 (1), 34–39.

[35] Hussein, M.Z., Hussein-Al-Ali, S., Zainal, Z., and Hakim, M., 2011, Development of antiproliferative nanohybrid compound with controlled release property using ellagic acid as the active agent, *Int. J. Nanomedicine*, 6, 1373–1383.

[36] Murtaza, G., Ahmad, M., and Shahnaz, G., 2010, Microencapsulation of diclofenac sodium by non-solvent addition technique, *Trop. J. Pharm. Res.*, 9 (2), 187–195.

[37] Kovanda, F., Maryšková, Z., and Kovář, P., 2011, Intercalation of paracetamol into the hydrotalcite-like host, *J. Solid State Chem.*, 184 (12), 3329–3335.

[38] Kong, X., Shi, S., Han, J., Zhu, F., Wei, M., and Duan, X., 2010, Preparation of Glycy-L-Tyrosine intercalated layered double hydroxide film and its *in vitro* release behavior, *Chem. Eng. J.*, 157 (2-3), 598–604.

[39] Hashim, N., Muda, Z., Abdul Hamid, S., Md Isa, I., Kamari, A., Mohamed, A., Hussein, M.Z., and Abd Ghani, S., 2014, Characterization and controlled release formulation of agrochemical herbicides based on zinc-layered hydroxide-3-(4-methoxyphenyl) propionate nanocomposite, *J. Phys. Chem. Sci.*, 1 (4), 1–6.

[40] Parello, M.L., Rojas, R., and Giacomelli, C.E., 2010, Dissolution kinetics and mechanism of Mg-Al layered double hydroxides: A simple approach to describe drug release in acid media, *J. Colloid Interface Sci.*, 351 (1), 134–139.

[41] Chang, H., Li, C., Huang, R., Su, R., Qi, W., and He, Z., 2019, Amphiphilic hydrogels for biomedical applications, *J. Mater. Chem. B*, 7 (18), 2899–2910.

[42] Prabhakar, K., Afzal, S.M., Surender, G., and Kishan, V., 2013, Tween 80 containing lipid nanoemulsions for delivery of indinavir to brain, *Acta Pharm. Sin. B*, 3 (5), 345–353.